ELSEVIER

Thermochimica Acta 373 (2001) 153–160

thermochimica acta

www.elsevier.com/locate/tca

Comments on "Calculation of the Energy of Transition Associated with Inversions in Double-Stranded DNA" [P. Aggarwal, D. Dollimore, Thermochim. Acta 284 (1996) 109]: a test

Richard Owczarzy*

Integrated DNA Technologies, 1710 Commercial Park, Coralville, IA 52241, USA

Received 15 December 2000; accepted 12 January 2001

Abstract

An alternative kinetic model of DNA melting curves, rising temperature kinetic evaluation, was recently suggested [Thermochim. Acta 284 (1996) 109] and applied to UV melting profiles of duplex DNA oligomers. We have investigated this kinetic model and compared it with the two-state thermodynamic equilibrium model. UV melting profiles for native DNA duplex oligomers were collected at various heating and cooling rates. Experimental melting curves of duplex DNA oligomers were found to be reversible and independent of the heating rates in range from 2.5 to 45°C h^{-1}. When the melting curves were evaluated in the terms of the alternative kinetic model, specific kinetic rate constants for duplex denaturation depended on the heating rates. These results indicate that native DNA duplex oligomers exhibit equilibrium melting transitions and the suggested kinetic model is invalid for melting profiles of native DNA duplex oligomers collected at the studied range of heating rates.

Keywords: DNA; Melting curve; Thermodynamics; Kinetic model

1. Introduction

Helix-coil transitions in DNA duplex oligomers can be monitored by ultraviolet absorbance at 268 nm while temperature of a sample is linearly increased. Recorded melting profiles (melting curves) of duplex DNA oligomers collected at heating rates up to 90°C h^{-1} are usually interpreted in terms of thermodynamic equilibrium model [2–6]. The sigmoidal shape of melting curves is a result of an equilibria mixture of melted (broken) and intact base pairs at a given temperature. A reasonable agreement between experimental melting curves and melting curves predicted from the corresponding thermodynamic equilibrium model was demonstrated numerous times [2,7–10].

By contrast, a kinetic interpolation of DNA melting curves was recently presented in this journal [1]. It was suggested that "a normal melting process is expected to occur at one temperature". Furthermore, it was proposed to apply a rising temperature kinetic model for DNA duplex melting transitions. Specifically, melting curves of duplex DNA oligomers in the paper [1] were interpreted in terms of Avrami–Erofeev kinetic expressions and Arhenius plots. The suggested kinetic model was originally used to describe kinetics of solid-state reactions, e.g. dehydratation, dehydroxylations, deammoniations, and other solid decompositions [11–16]. Avrami–Erofeev kinetic equations are

* Fax: +1-319-626-8444.
E-mail address: rowczarzy@idtdna.com (R. Owczarzy).

0040-6031/01/$ – see front matter
PII: S0040-6031(01)00460-9

derived from the geometry of the solid-state reaction interface and are often applied to heterogeneous systems. However, validity of this kinetic model for DNA melting profiles remains to be determined. Such assessments require melting data on DNA duplex oligomers collected at various heating rates as well as melting data for DNA denaturation and renaturation. Because the suggested kinetic interpolation of DNA melting curves is in disagreement with the thermodynamic equilibrium model, we examined both models and collected melting data at various heating rates. Results of melting experiments were compared with the tested kinetic model [1] and the two-state thermodynamic model [2,6,17] of DNA melting curves.

2. Theory

Details of thermodynamic equilibrium model of DNA melting curves were published elsewhere [2,4,6,17]. To briefly review an extraction of transition enthalpies and entropies from experimental melting curves, let us consider melting of duplex oligomer, D, to two different single strands, S_1, S_2;

$$D \rightleftharpoons S_1 + S_2$$

Concentration of single strands is typically same, $[S_1] = [S_2]$. The fraction of melted duplexes, θ, is then defined to be,

$$\theta = \frac{[S_1] + [S_2]}{2[D] + [S_1] + [S_2]} = \frac{[S_1]}{[D] + [S_1]} = \frac{2[S_1]}{C_t} \tag{1}$$

where $C_t = [S_1] + [S_2] + 2[D]$ is the total single strand concentration of oligonucleotides. Using an assumption of two-state transition and zero heat capacity change during equilibrium melting transition, van't Hoff transition enthalpies, ΔH, can be determined from the maxima of derivative melting curves, $d\theta/dT$ versus T [17,18],

$$\Delta T = 6RT_m^2 \left[\frac{d\theta}{dT}\right]_{max} \tag{2}$$

where R is the ideal gas constant and T_m is the melting temperature. Corresponding transition entropies for duplex denaturation, ΔS, are estimated [19] from

$$\Delta S = \frac{\Delta H}{T_m} + R\ln\left(\frac{C_t}{4}\right) = 6RT_m\left[\frac{d\theta}{dT}\right]_{max} + R\ln\left(\frac{C_t}{4}\right) \tag{3}$$

Assuming bimolecular two-state melting transition, the relationship between the denaturation equilibrium constant, K_d, and θ is [6,20],

$$K_d = \frac{[S_1][S_2]}{[D]} = \frac{\theta^2}{2(1-\theta)}C_t \tag{4}$$

Solution of Eq. (4) yields an expression used for prediction of DNA melting profiles from the ΔH, ΔS values,

$$\theta = \frac{\sqrt{K_d^2 + 2C_tK_d} - K_d}{C_t} \tag{5}$$

where

$$K_d = \exp\left(-\frac{\Delta H - \Delta S\,T}{RT}\right)$$

Eq. (5) describes melting transitions of duplexes formed from two *different* single strands, i.e. non-self-complementary strands. A different equation is derived for a duplex formed from a self-complementary oligomer [3]. It should be stressed that in this comment, ΔH and ΔS refer to standard molar transition enthalpies and entropies for duplex *melting* (helix to coil process).

Alternatively, Aggarwal and Dollimore suggested a new approach to interpretation of DNA melting curves, the kinetic interpolation of DNA melting curves [1]. Assuming linear heating rate β, they derived a kinetic equation,

$$\left[\frac{d\theta}{dT}\right]\beta = k(T)f(\theta) \tag{6}$$

where $k(T)$ is a specific reaction rate constant at a given temperature T, and θ is the extent of reaction, which is the fraction of broken base pairs in case of DNA duplexes. The function of $f(\theta)$ was proposed to have a form of either Avrami–Erofeev equation,

$$f(\theta) = n(1-\theta)[-\ln(1-\theta)]^{1-(1/n)} \tag{7}$$

where $n = 2, 3, 4$, or second-order reaction,

$$f(\theta) = (1-\theta)^2 \tag{8}$$

The correct assignment of the form of $f(\theta)$ was judged from the correlation coefficients obtained in the Arhenius plots of $\ln k(T)$ versus $1/T$,

$$\ln k(T) = \ln A - \frac{E_a}{RT} \quad (9)$$

where A is the pre-exponential term, and E_a is the activation energy. We followed strictly the published procedure [1]. Parts of melting curves having θ from 0.2 to 0.8 were employed to derive $k(T)$, A, and E_a values.

3. Experimental methods

DNA oligomers were synthesized using standard phosphoramidite method (Integrated DNA Technologies), deprotected and desalted on NAP-5 columns (Amersham Pharmacia Biotech). Oligomers were purified using 20% polyacrylamide gel electrophoresis in 1× TBE buffer (85 mM Tris, 85 mM boric acid, 1 mM Na_2EDTA). The purity of oligomers was determined by capillary electrophoresis (CE) carried out on Beckman PACE 5000. CE capillary had 100 μm inner diameter and contained ssDNA 100R Gel (Beckman-Coulter). Typically, about 0.6 nmol of oligonucleotide was injected, ran in electric field of 444 V cm^{-1} and detected by UV absorbance at 260 nm. Denaturing Tris-borate-7M-urea running buffer was purchased from Beckman–Coulter. CE assays indicated that all oligomers were more then 95% pure. Molar masses of oligomers were determined on MALDI TOF Voyager DE mass spectrometer. Experimental molar masses of all oligomers were within 0.4% of expected molar masses. Melting experiments were carried out in the buffer containing 50 mM NaCl, 3.87 mM NaH_2PO_4, 6.13 mM Na_2HPO_4, 1 mM Na_2EDTA, pH = 7.0 adjusted with NaOH. Total Na^+ concentration was estimated to be 68.8 mM. DNA samples were thoroughly dialyzed against melting buffer in QuixSep microdialyzers (Membrane Filtration Products). Concentrations of DNA oligomers were determined from absorbance at 260 nm and estimated extinction coefficients, which were calculated using nearest-neighbor model [21–23]. Oligomer concentrations were estimated at least twice for each sample. If the oligomer concentrations differed more then 4%, the results were discarded and new absorbance measurements were done. To prepare duplexes, complementary DNA oligomers were mixed in 1:1 molar ratio, heated to 92°C and slowly cooled down to an ambient temperature.

DNA solutions were diluted with the melting buffer to absorbance of 0.45 and degassed by applying a vacuum in Speed-Vac concentrator for less than 10 s. Measurements of mass showed insignificant amounts of buffer evaporation (less than 0.4%) during degassing. Melting experiments were conducted on a single beam Beckman DU 650 spectrophotometer (Beckman–Coulter) with a Micro Tm Analysis accessory, Beckman High Performance Peltier Controller, and 1 cm path-length cuvettes. Because original software had rather limiting features, melting data were recorded by our TmColl program that ran on a PC interfaced to the spectrophotometer. The spectrophotometer was switched into a program mode and controlled by a macro. Absorbance values at 268 nm were measured every 0.1°C in the temperature range of 15–85°C. Both heating (denaturation) and cooling (renaturation) transition curves were recorded at four rates of temperature change, specifically at 2.46 ± 0.05, 9.87 ± 0.07, 24.9 ± 0.1 and 45.8 ± 0.1°C h^{-1}.

Melting profiles of buffers alone were also collected in the same sample cuvettes and subtracted digitally from raw melting curves of DNA samples. Melting experiments were analyzed as described earlier [3]. The fraction of broken base pairs, θ, was calculated from the graph of raw absorbance versus temperature [2,18]. The transition curves were smoothed by digital filter [24]. Reported transition (melting) temperatures, T_m's, are temperatures where the derivative curve, $d\theta/dT$ versus temperature, reaches the maximum. Experimental T_m's were reproducible within 0.3°C. At least two melting curves were collected for each heating and cooling experiment in different cuvettes and in different positions inside of the Peltier holder to minimize systematic errors. Initially, thermistor thermometer 874C with type K thermocouple (Tegam, Inc.) was employed to measure temperatures directly inside of the cuvettes. The differences between the temperatures recorded by the external probe immersed into DNA solution and the temperatures reported by the internal probe located inside of the cell holder were less then 0.4°C. These temperature differences are close to the error of temperature probes. Hence, only temperatures from the internal probe located

Table 1
Sequences and their estimated extinction coefficients

Duplex	Complementary sequences (5′–3′)	Extinction coefficient (l mol^{-1} cm^{-1})
I	AGTAGTAATCACACC	154.3×10^3
	GGTGTGATTACTACT	145.0×10^3
II	CCACTATACCATCTATGTAC	189.7×10^3
	GTACATAGATGGTATAGTGG	211.3×10^3
III	TCCACACGGTAGTAAAATTAGGCTT	247.2×10^3
	AAGCCTAATTTTACTACCGTGTGGA	244.5×10^3

inside of the Peltier holder were subsequently recorded. The external temperature probes seem to be redundant due to unique design of the Beckman cell holder and small volumes of solutions in cuvettes (365 μl).

4. Results and discussion

4.1. Dependence of melting temperatures and melting profiles on the heating rates

The alternative kinetic model [1] was demonstrated on melting profiles of 16 bp deoxyoligonucleotides [25] and 13-mer duplex [19] collected at heating rates of 18 and 30°C h^{-1}, respectively. To examine this kinetic model, we studied three duplexes of similar length and recorded their ultraviolet thermal denaturation and renaturation profiles at rates of temperature change, β, ranging from 2.5 to 46°C h^{-1}. The synthetic DNA oligomers in this study have GC content of 40% and are shown in Table 1. Extinction coefficients of deoxyoligonucleotides were estimated using nearest-neighbor model as described in Section 3. The length of studied duplexes varied from 15 to 25 bp.

Melting temperatures determined from denaturation and renaturation curves are summarized in Table 2. The experimental melting temperatures are insensitive to the rate of temperature change in the range of 2.5–46°C h^{-1}. This result is consistent with thermodynamic equilibrium model of melting curves and is conflicting with proposed kinetic model. When the melting curve is collected under non-equilibrium conditions, DNA oligomer will melt at temperature, T_k, which is higher then T_m [2]. The difference, $T_k - T_m$, is then increasing with increasing β. No such behavior is observed for studied duplexes. By contrast, experimental melting temperatures determined from denaturation and renaturation curves are same within the error of experiment and independent of the rate of temperature change. This result suggests equilibrium conditions throughout melting process. Inspection of Table 2 reveals that at reported DNA concentrations, average T_m's are 46.1, 53.0, 61.1°C for duplex I, II, III, respectively.

Table 2
Dependence of melting temperatures determined from denaturation and renaturation curves on rates of temperature changes, β

Duplex	C_t (μM)	Helix-coil transition	Average melting temperature (°C) at the rate of temperature change			
			2.46°C h^{-1}	9.87°C h^{-1}	24.9°C h^{-1}	45.8°C h^{-1}
I	3.3	Denaturation	46.2	46.1	46.1	46.2
		Renaturation	46.1	46.2	46.0	45.8
II	2.6	Denaturation	53.0	53.0	53.2	53.1
		Renaturation	53.1	53.0	52.9	52.9
III	2.0	Denaturation	61.1	61.2	61.4	61.5
		Renaturation	61.1	61.1	61.0	60.8

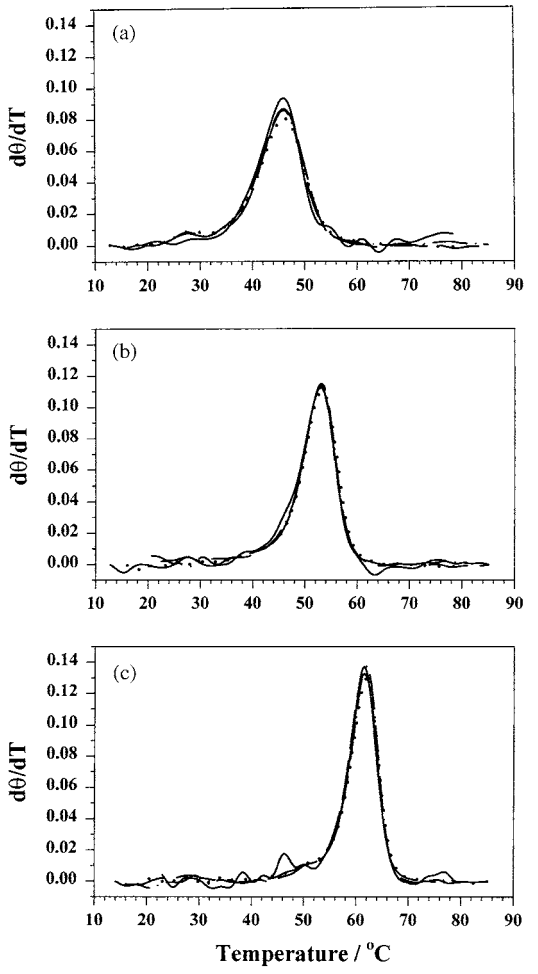

Fig. 1. Experimental derivative *denaturation* curves, plots of $d\theta/dT$ vs. T, for duplex I (a), duplex II (b), and duplex III (c) at four different heating rates, 2.46 (solid line), 9.87 (dash line), 24.9 (dash-dot-dash line), and 45.8 °C h^{-1} (dotted line).

Dependence of derivative denaturation curves, the plots of $d\theta/dT$ versus T, on the heating rate is shown on Fig. 1. Within the errors of $d\theta/dT$ (0.005), shapes of the denaturation curves and maxima of $d\theta/dT$ were found to be independent of rates of temperature change. These observations are consistent with the equilibrium transitions and inconsistent with the proposed kinetic model. If the melting curves had been collected under non-equilibrium conditions, shapes of the derivative melting curves would have varied with increasing β and maxima of $d\theta/dT$, $[d\theta/dT]_{max}$, would have been shifted to higher temperatures. Average $[d\theta/dT]_{max}$ was 0.087 ± 0.005 for duplex I, 0.113 ± 0.005 for duplex II, and 0.137 ± 0.004 for duplex III, respectively. The value of $[d\theta/dT]_{max}$ is independent of β but is increasing with the length and thermal stability of duplexes.

4.2. Reversibility of helix-coil transitions

Denaturation and renaturation curves collected at $\beta = 2.47$, 9.87, 24.9 and 45.8°C h^{-1} are shown on Fig. 2. When changing temperature at those rates,

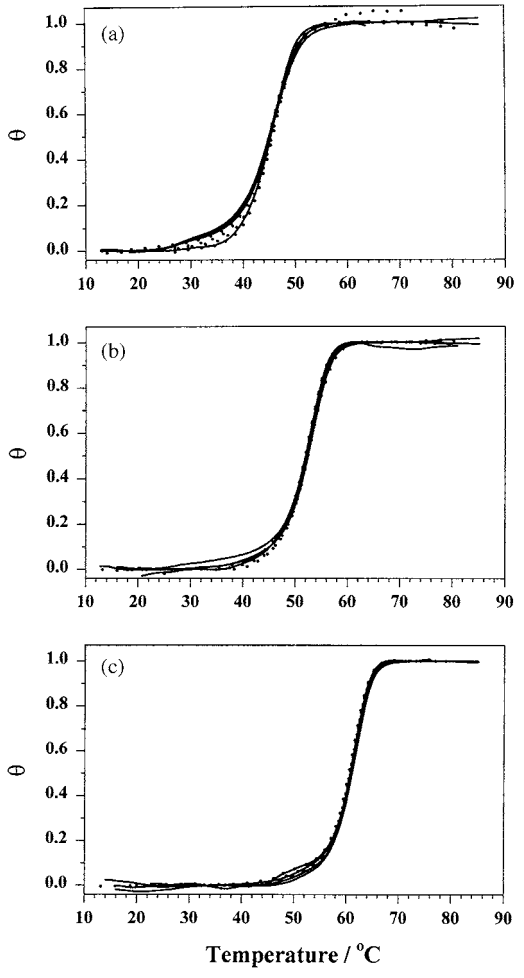

Fig. 2. Denaturation (solid lines) and renaturation (dotted lines) transition curves for duplex I (a), duplex II (b), and duplex III (c) collected at $\beta = 2.46$, 9.87, 24.9, and 45.8°C h^{-1} are plotted on the same scale.

melting transitions of 15, 20, and 25 bp long duplex DNAs were found to be reversible in 69 mM Na^+ buffer. In other words, examination of Fig. 2 reveals that denaturation and renaturation curves overlap within the error of experiment. No significant hysteresis between denaturation and renaturation curves was detected. These results indicate that thermal equilibrium was established throughout studied melting transitions. Such reversibility of melting profiles of native DNA duplex oligomers was observed in other laboratories. For example, DNA melting transitions were reported to be reversible for more then hundred of 6–25 bp long duplexes in buffers of ionic strength ranging from 115 mM to 1.0 M Na^+ [3,26–29].

4.3. Comparison between suggested kinetic model and thermodynamic equilibrium model

For duplexes I–III, UV denaturation and renaturation profiles were interpreted in terms of both kinetic and thermodynamic models. Results of two-state thermodynamic equilibrium model are shown on the left side of Table 3. Results of alternative kinetic model are presented on the right side of Table 3. Higher correlation coefficients of Arhenius plots were obtained when kinetic model functions $f(\theta)$ had a form of second-order Eq. (8). Thus, the Eq. (8) was preferred to Avrami–Erofeev Eq. (7). Relative errors of ΔH, ΔS, $\ln k(T)$, and E_a were estimated to be 7, 8, 17, and 2%, respectively. The errors were propagated from errors of T_m's and $d\theta/dT$ [30]. In terms of the thermodynamic model, experimental values of transitions enthalpies and entropies determined from Eqs. (2) and (3) do not depend on the rate of temperature change, as expected. Furthermore, transition enthalpies and entropies were estimated from a nearest-neighbor thermodynamic model and SantaLucia set of parameters [31]. Estimated ΔH's are 458, 623, and 796 kJ mol^{-1} for duplex I–III, respectively. Transition entropies were estimated to be 1.33, 1.81, and 2.27 kJ mol^{-1} K^{-1} for duplex I–III, respectively. Comparison reveals that the predicted transition enthalpies and entropies from nearest-neighbor thermodynamic model show excellent agreement with the experimental transition enthalpies and entropies.

In terms of the alternative kinetic model, activation energies are insensitive to β. Interestingly, evaluated specific reaction rate constants, $k(T)$, increase about 20 times when β is increased from 2.5 to 46°C h^{-1}. For example, at $\beta = 2.5$°C h^{-1}, k (46.1°C) is 2.86×10^{-4} for duplex I, but at $\beta = 46$°C h^{-1}, k (46.1°C) is 59.2×10^{-4}. This result of the proposed kinetic model is in discrepancy with the assumed properties of $k(T)$. The specific reaction rate constant is assumed to be constant at a given temperature T and insensitive to β or extent of reaction. Analysis of Eq. (9) can shed light on this discrepancy. Combination of Eqs. (6) and (9) yields

$$\ln\left[\frac{d\theta}{dT}\right] - \ln[f(\theta)] + \ln\beta = \ln A - \frac{E_a}{RT} = \ln k(T) \tag{10}$$

Table 3
Results of thermodynamic and kinetic interpolations of denaturation (melting) curves at various heating rates, β[a]

Duplex	β (°C h^{-1})	ΔH (kJ mol^{-1})	ΔS (kJ mol^{-1} K^{-1})	$-\ln k(T_m)$	E_a (kJ mol^{-1})
I	2.46	476	1.38	8.16	333
	9.87	440	1.26	6.59	326
	24.9	435	1.25	5.60	331
	45.8	409	1.16	5.13	302
II	2.46	597	1.71	7.52	444
	9.87	605	1.74	6.17	452
	24.9	615	1.76	5.32	455
	45.8	590	1.69	4.87	434
III	2.46	794	2.26	7.77	567
	9.87	758	2.15	6.34	553
	24.9	775	2.19	5.50	573
	45.8	739	2.09	4.96	543

[a] Specific rate constants, $k(T)$, are reported at T_m's, i.e. at 46.1, 53.0, 61.1°C for duplex I–III, respectively.

Because collected melting transitions were independent of β, the first two terms on the left side of Eq. (10) were found to be independent of β for a given duplex. Additionally, β was constant for each melting profile and independent of temperature. Therefore, the third term on the left side, ln β, causes increase of ln $k(T)$ with increasing β, but this term has no influence on the value of E_a.

It was argued that in a normal melting process, the melting phenomenon is expected to occur at one temperature [1]. That does not seems to be case for DNA duplex oligomers, which exhibit sigmoidal shape of melting curve even for equilibrium transitions. Assuming two-state model, the sigmoidal melting profiles can be predicted from transition enthalpies and entropies using Eq. (5). We employed transition enthalpies and entropies from Table 3 to calculate helix-to-coil transition profiles of duplex I–III. For all three duplexes, predicted transition profiles overlapped with experimental denaturation and renaturation profiles (data not shown). Hence, the sigmoidal shape of DNA denaturation and renaturation curve is not an indication of non-equilibrium process. We believe that for DNA duplex oligomers, the significant fraction of the broken base pairs coexists in equilibrium with the intact base pairs even several degrees below melting temperature. Analogously, the significant fraction of intact base pairs may be detected at temperatures above T_m. Slight deviations of experimental profiles from predicted melting profiles may result from non-two-state behavior or subtle changes in base-stacking and average secondary structure with temperature.

5. Conclusions

This short study was conducted with the goal of testing suggested rising temperature evaluation of DNA melting profiles [1]. Ultraviolet denaturation and renaturation profiles of DNA duplex oligomers were collected at various heating rates in the range from 2.5 to 46°C h^{-1}. Results reveal that the suggested kinetic model of DNA melting curves [1] is in discrepancy with several observed phenomena. First, the denaturation and renaturation curves overlap and are independent of the rate of temperature change in the range from 2.5 to 46°C h^{-1}. Second, the same transition temperatures, T_m, (within the error of experiment) are determined from denaturation and renaturation curves collected at studied β's. These results suggest the DNA solutions are closed to the thermodynamic equilibrium. It seems that for native DNA duplex oligomers up to 25 bp long, kinetics of duplex denaturation and renaturation is fast enough to bring the duplex and single strands close to the thermodynamic equilibrium in the usual range of studied heating rates, buffer and DNA concentrations.

Mathematical functions of Avrami–Erofeev equation (Eq. (7)) and second-order equation (Eq. (8)), $f(\theta)$, can interpolate various sigmoidal curves. Studied melting curves of DNA duplex oligomers could be ostensibly interpolated by kinetic equations of Avrami–Erofeev or second-order equations, but such interpolations result in values of A, ln k, and E_a, which seem to have no physicochemical meaning. Our observations indicate that the melting process of duplex DNA oligomers is in equilibrium under these conditions and the sigmoidal shape of the denaturation curves does not depend on kinetics. Therefore, we believe that the rising temperature kinetic evaluation should not be applied for melting profiles of duplex DNA oligomers at these heating rates, and the activation energies and the specific reaction rates reported in Table 1 of the paper [1] and Table 3 of this comment are of little value. The author suggests that any melting study of DNA duplexes measures both denaturation and renaturation curves to test equilibrium conditions of helix-coil transitions.

Acknowledgements

I wish to thank Lisa Bogh for determination of DNA purity by capillary electrophoresis. Thank Brian Elliott and Shawn Eyestone for mass spectroscopy measurements.

References

[1] P. Aggarwal, D. Dollimore, Thermochim. Acta 284 (1996) 109.
[2] R.M. Wartell, A.S. Benight, Phys. Rep. 126 (1985) 67.
[3] R. Owczarzy, P.M. Vallone, F.J. Gallo, T.M. Paner, M.J. Lane, A.S. Benight, Biopolymers 44 (1997) 217.
[4] K.J. Breslauer, Methods Enzymol. 259 (1987) 221.

[5] H.T. Allawi, J. SantaLucia Jr., Biochemistry 36 (1997) 10581.
[6] M. Petersheim, D.H. Turner, Biochemistry 22 (1983) 256.
[7] O. Gotoh, Y. Tagashira, Biopolymers 20 (1981) 1033.
[8] A. Wada, S. Yabuki, Y. Husimi, CRC Critic. Rev. Biochem. 9 (1980) 87.
[9] B.R. Amirikyan, A.V. Vologodskii, Y.L. Lyubchenko, Nucl. Acids Res. 9 (1981) 5469.
[10] A.S. Benight, R.M. Wartell, D.K. Howell, Nature 289 (1981) 203.
[11] A.R. Salvador, E.G. Calvo, Thermochim. Acta 203 (1992) 67.
[12] J. Malek, J.M. Criado, Thermochim. Acta 203 (1992) 25.
[13] D. Dollimore, T.A. Evans, Y.F. Lee, F.W. Wilburn, Thermochim. Acta 188 (1991) 77.
[14] D. Dollimore, Thermochim. Acta 203 (1992) 7.
[15] H. Tanaka, Thermochim. Acta 267 (1995) 29.
[16] M. Alonso, B. Lopez-Delgado, F.A. Lopez, J. Mater. Sci. 33 (1998) 5821.
[17] L.A. Marky, K.J. Breslauer, Biopolymers 26 (1987) 1601.
[18] J.W. Nelson, F.H. Martin, I. Tinoco Jr., Bipolymers 20 (1981) 2509.
[19] G.E. Plum, A.P. Grollman, F. Johnson, K.J. Breslauer, Biochemistry 31 (1992) 12096.
[20] E.M. Evertsz, K. Rippe, T.M. Jovin, Nucl. Acids Res. 22 (1994) 3293.
[21] G.D. Fasman, Handbook of Biochemistry and Molecular Biology, Vol. I, CRC Press, Boca Raton, 1975, pp. 589.
[22] C.R. Cantor, M.M. Warshaw, Biopolymers 9 (1970) 1059.
[23] G. Kallansrud, B. Ward, Anal. Biochem. 236 (1996) 134.
[24] J.F. Kaiser, W.A. Reed, Rev. Sci. Instrum. 48 (1977) 1447.
[25] R.D. Sheardy, N. Levine, S. Marotta, D. Suh, J.B. Chaires, Biochemistry 33 (1994) 1385.
[26] M.J. Doktycz, M.D. Morris, S.J. Dormady, K.L. Beattie, K.B. Jacobson, J. Biol. Chem. 270 (1995) 8439.
[27] K. Bolewska, A. Zielenkiewicz, K.L. Wierzchowski, Nucl. Acid Res. 12 (1984) 3245.
[28] I. Pompizi, A. Häberli, C.J. Leumann, Nucl. Acid Res. 28 (2000) 2702.
[29] A. Schöppe, H-J. Hinz, H. Rosemeyer, F. Seela, Eur. J. Biochem. 239 (1996) 33.
[30] P.R. Bevington, D.K. Robinson, Data Reduction and Error Analysis for the Physical Sciences, WCB/McGraw-Hill, Boston, 1992, p. 42.
[31] J. SantaLucia Jr., Proc. Natl. Acad. Sci. U.S.A. 95 (1998) 1460.